Multi-Qubit Quantum Chip Modeling: From Device Design to Realistic Quantum Dynamics Simulation

Ngawang Rigdol, Damilola Babajide, Wesley Ihezuo

July 2025

1 Abstract

This project aims to create a simulation framework for multi-transmon-qubit quantum chips by designing/modeling and simulating quantum dynamics. Starting with the simulation of a single transmon qubit, and then later coupling it to a microwave resonator, we extract key physical parameters including resonant frequencies, qubit lifetimes (T1 and T2), dispersive shifts, and photon number evolution. We start the simulation by sending a Gaussian pulse to our resonator. Using QuTiP, we model the energy spectrum (eigenenergies) and time evolution of the coupled system, incorporating decoherence effects as well via collapse operators to simulate realistic quantum behavior. The ultimate goal is to extend this simulation to multi-qubit systems containing six or more transmons coupled to one resonator. To enhance realism, we plan to use Ansys HFSS to extract important key data about our quantum chip, such as its resonant frequencies, EJ and EC values. We then plan to input these values into QuTiP to do the real simulation/analysis work to obtain real and raw data. This project is aiming to simulate a quantum chip as realistically as possible, given the software on deck.

2 Introduction

Superconducting qubits have emerged as one of the leading platforms for scal- able quantum computing. Their integration with coplanar waveguide

resonators allows for complex architectures and tunable interactions between qubits. In this project, we modeled and simulated a superconducting quantum chip com- posed of transmon qubits using tools like Qiskit Metal, QuTiP, and Ansys. Our chip consists of six fixed-frequency transmon qubits and one central flux- tunable transmon qubit, connected via two superconducting coplanar waveguides (CPW) resonators. The two key components of a superconducting qubit, such as a Transmon qubit, is the Josephson Junction and a shunt capacitor. Joseph- son Junctions is an insulator sandwiched between two pads of superconducting plates, causing a non-linear quantum harmonic oscillator to form, which gives birth to our two level system (Transmon qubit). A qubit is just one compo- nent in a quantum chip, there are many more such as resonators, drive lines, readouts, etc. The couplingstrength denoted by g determines how strongly two quantum systems interact1 and exchange energy. The coupling strength of the two quantum systems can be between the transmon qubit and a microwave resonator. The two systems exist independently of each other if no coupling element is present, meaning their energy levels cross over and don't affect one another. Once we add a coupling element, and g is very large, the two systems will now become entangled, splitting and forming new hybridized energy levels. The coupling strength also changes the resonant frequencies of the transmon, due to the new hybridized energy levels. Resonant frequencies are important be- cause it tells you the exact freuency that you need to send a EM pulse to excite a qubit. Qubit lifetimes are denoted either by T1 or T2, depending on if you 8 want to measure it's excitation decay rate, (time taken for the qubit to fall from it's excited state back to the ground state denoted by T1), or it's decoherence rate, (the time taken for a qubit to lose it's quantum properties denoted by T2). We have covered most of the important key aspects of a meaningful quantum chip simulation, and will proceed to go on with the experiments. The purpose of our work was to better understand the energy spectra, connectivity, and dy- namics of this multi-qubit system, and to see how design changes could impact performance. We focused on modeling the transmon Hamiltonians, visualizing the quantum chip layout, and simulating coupled dynamics between the qubits and resonators. This kind of research is important as quantum hardware scales up, and it gives us experience in the full stack of quantum development—from device design to simulation.

3 Related Work

A lot of our research is based on famous models like the Jaynes cumming and Tavis cumming Model. These models showcase the interactions between qubits and resonators. Companies like IBM have developed chips with similar layouts that use a central tunable qubit to improve communication between fixed-frequency qubits. One of the big reasons for doing this is to avoid frequency collisions, which can mess up gate operations. Qiskit Metal is commonly used to design these chips, and QuTiP makes it easier to simulate the quantum mechanics involved, especially for energy level calculations and time evolution. We followed this approach because it's well-tested and lines up with what other people have done in the field.

4 Preliminary Data

We have simulated a quantum chip containing a single transmon qubit coupled to a resonator using ElmerFEM (Alternative to Ansys). We extracted important properties of the qubit such as the inverse capacitance and inductance matrices, which is needed to calculate the EJ and EC values.

The Hamiltonian of the transmon qubit is given by:

$$H_{\text{transmon}} = 4E_C(n - n_g)^2 - E_J \cos\phi, \tag{1}$$

where E_C is the charging energy, E_J is the Josephson energy, and n_g is the offset charge.

The simulation gave the values for our parameters $E_C = 0.3$ GHz, $E_J = 12$ GHz, and $n_g = 0$. Using QuTiP, we computed the resonant frequency of our transmon qubit, (energy needed to jump from the ground to the first excited state).

$$f_{01} = 5.9346 \text{ GHz}.$$

We implemented a resonator to our chip next. The resonator has Hamiltonian:

$$H_{\text{res}} = \hbar\omega_r a^\dagger a, \tag{2}$$

where ω_r is the resonator frequency.

The total Hamiltonian including the interaction term (Coupling effects between the transmon and resonator) is:

$$H = H_{\text{transmon}} + H_{\text{res}} + H_{\text{int}}, \quad H_{\text{int}} = \hbar g(a^\dagger|0\rangle\langle 1| + a|1\rangle\langle 0|), \tag{3}$$

where g denotes the coupling strength between the transmon and the resonator.

Hybridization Due to Qubit-Resonator Coupling

We then coupled the transmon qubit to the single-mode microwave resonator (the one we just implemented) modeled as a harmonic oscillator, with $\omega_r = 7$ GHz.

The full system Hamiltonian is:

$$H = H_{\text{transmon}} \otimes I + I \otimes H_{\text{res}} + H_{\text{int}}, \tag{4}$$

where the interaction Hamiltonian takes the Jaynes-Cummings form as previously mentioned:

$$H_{\text{int}} = \hbar g \left(a^\dagger |0\rangle\langle 1| + a|1\rangle\langle 0| \right), \tag{5}$$

with the coupling strength $g = 0.005$ GHz.

The lowest energy transitions and anharmonicity were revealed to be:

$$f_{01} = 5.9346 \text{ GHz}, \quad f_{12} = 1.0655 \text{ GHz}, \quad \text{Anharmonicity} = -4.8691 \text{ GHz}.$$

Driven Resonator Dynamics

We applied a Gaussian drive pulse to the resonator mode. The time-dependent drive Hamiltonian is:

$$H_{\text{drive}}(t) = \Omega(t)(a + a^\dagger), \tag{6}$$

where the pulse envelope is

$$\Omega(t) = \Omega_0 \exp\left(-\frac{(t - t_0)^2}{2\sigma^2} \right),$$

with amplitude $\Omega_0 = 0.05$, pulse duration $t_{\text{drive}} = 500$ ns, center $t_0 = t_{\text{drive}}/2$, and width $\sigma = t_{\text{drive}}/6$.

We solved the master equation using QuTiP's `mesolve` including this drive. The resonator photon number $\langle a^\dagger a \rangle$ was observed to rise during the pulse, proving that the pulse worked, and then dropping back down, showing dissipation.

Qubit Decoherence and Dissipation

To include qubit relaxation (time it takes to go back down to the ground state) and dephasing (coherence decay), we added collapse operators:

$$c_1 = \sqrt{\gamma_1}\,\sigma_-, \quad c_\phi = \sqrt{\gamma_\phi}\,\sigma_z,$$

where $\gamma_1 = 1/T_1$ with $T_1 = 30$ ns and $\gamma_\phi = 1/T_2 - \frac{1}{2T_1}$ with $T_2 = 40$ ns.

Including these dissipative processes in the simulation showed the resonator photon number decaying in time, along with the qubit excited state population, reflecting energy relaxation and dephasing effects in the system.

Dispersive Shift and Qubit-State-Dependent Resonator Response

The dispersive shift is how much the resonator changes in frequency depending on the state of the qubit. The dispersive shift is calculated as:

$$\chi = \frac{g^2}{\Delta} \approx -1.0654 \text{ GHz}.$$

where $\Delta = \omega_q - \omega_r$,

and $\omega_q \approx 5.9346$ GHz (qubit transition frequency) and $\omega_r = 7.0$ GHz.

We performed readout simulations by applying Gaussian pulses at frequencies

$$\omega_{r,0} = \omega_r - \chi, \quad \omega_{r,1} = \omega_r + \chi,$$

corresponding to the resonator frequency shifted by the qubit being in the ground ($|0\rangle$) or excited ($|1\rangle$) state, respectively.

The time evolution of the resonator photon number $\langle a^\dagger a \rangle$ was simulated for both initial qubit states. The resonator's photon count clearly does not differ depending on the qubit state, which leaves questions to what kind of error may have occured during this experiment, as the plot should not have been the same.

4.1 Design

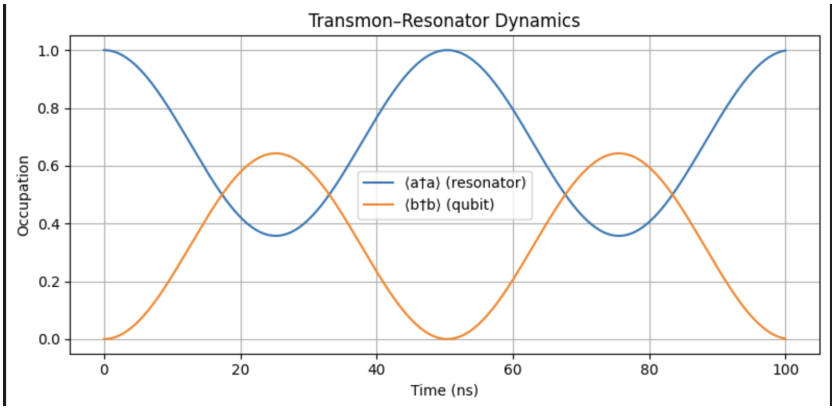

Figure 1: The Jaynes Cumming Model shows the interacting between a qubit and a resonator. In these models, the energy constantly moves between the qubit and the resonator, so we see excitations swapping back and forth.

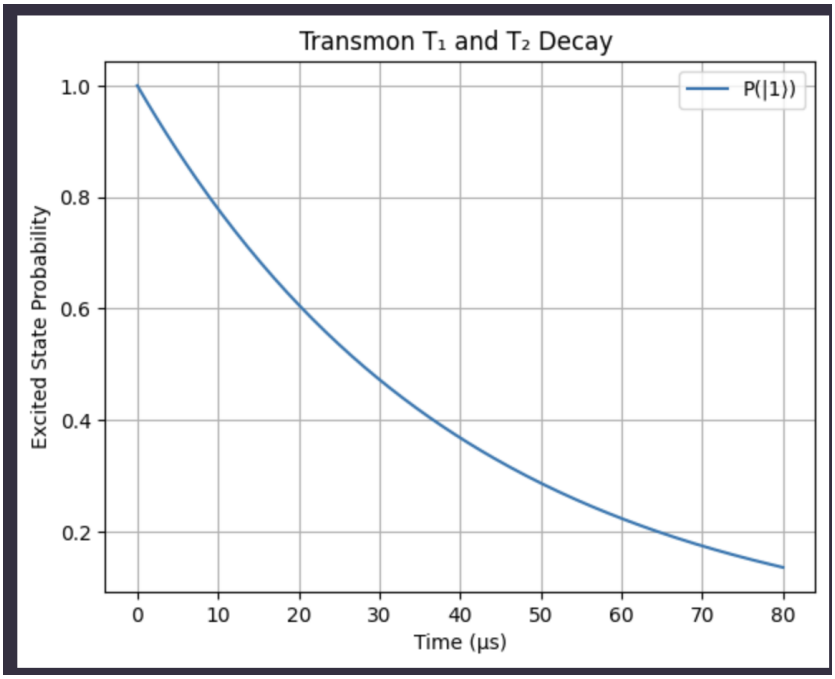

Figure 2: This figure shows the qubit lifetime of a transmon qubit with an E_J value of 15 GHz, E_C value of 300 MHz, a T_1 value of 40 μs, and a T_2 value of 60 μs.

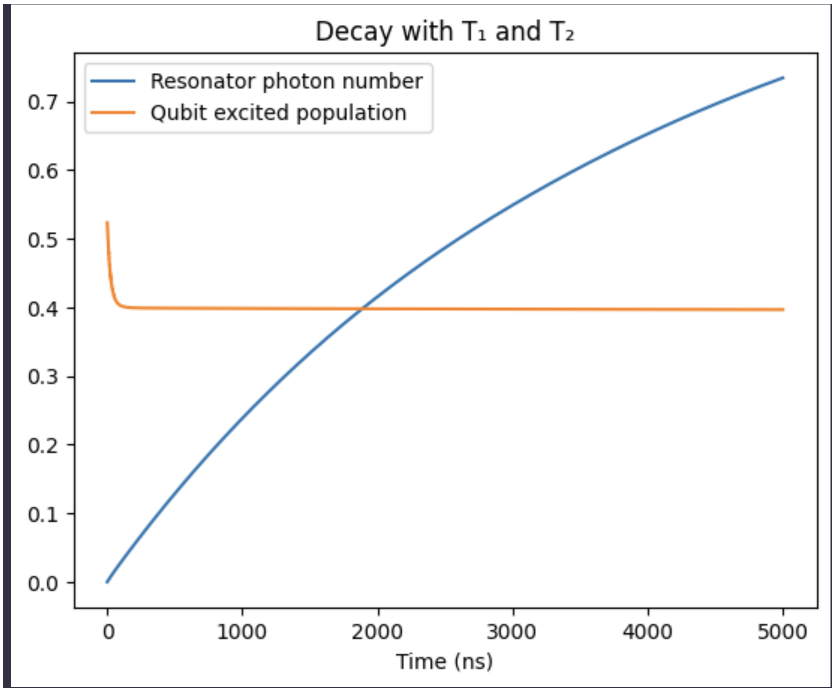

Figure 3: Simulated decay of a transmon qubit coupled to a resonator, showing the resonator photon number and the qubit excited-state population over time.

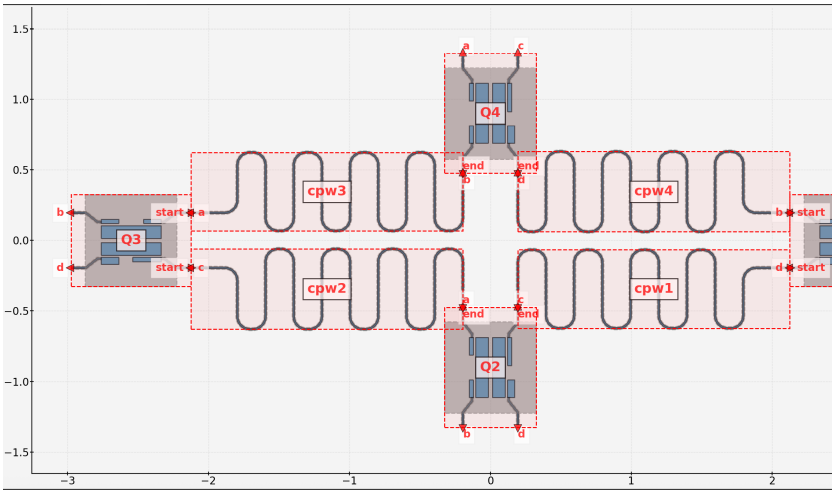

Figure 4: Design layout of a four-transmon qubit device with each qubit(Q1–Q4) coupled to its dedicated coupling resonator(CPW1–CPW4).

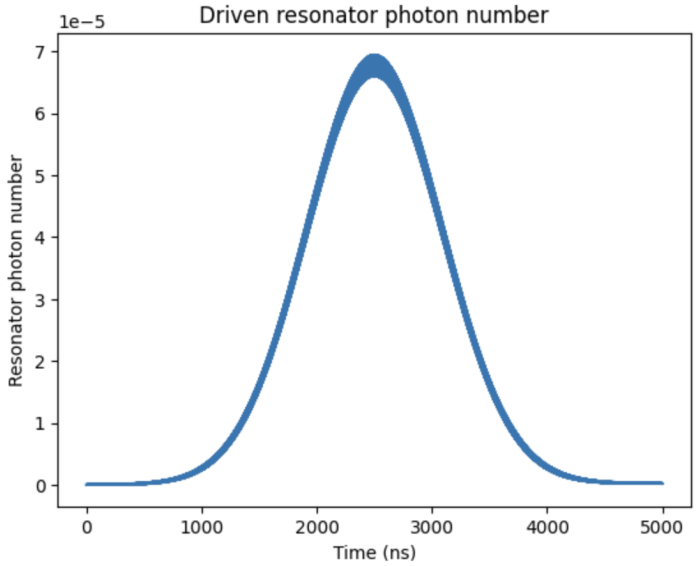

Figure 5: Time evolution of the driven resonator photon number. The curve shows the photon population in the resonator as a function of time, peaking around 250 ns.

Conclusion

We now begin our actual quantum chip design, and plan to use all of these equations and simulations for our chip. The chip's observables will be extracted using a EM simulation tool, and then plugging in the observables into the hamiltonians as seen above to extract real data from a custom made chip design.

5 Methodology

To model and analyze the 7 qubit superconducting quantum chip, we used a combination of softwares like Qiskit Metal, QuTiP, ElmerFEM, and Gmsh. These softwares enabled us to create realistic device design, electromagnetic modeling, and quantum simulation in a single process.

We began by using Qiskit Metal to design and visualize the layout of the chip. The architecture consists of 7 fixed-frequency transmon qubits and one central transmon, each coupled to individual or shared resonators. Each qubit was specified by geometric factors such as junction width, pad size, and spacing. We extract the capacitance matrix from the layout to describe coupling strengths and influence the Hamiltonian formula.

Using the extracted parameters, we modeled the device using both Jaynes-Cummings and Tavis-Cummings Hamiltonians. The resonator-qubit interactions were defined by the Jaynes-Cummings model, while the collective behavior of the multi-qubit system was captured using the Tavis-Cummings framework. In particular,we looked at the interaction Hamiltonian:

$$H_{\text{int}} = \sum_{j=1}^{N} g_j \left(a^\dagger \sigma_j^- + a\, \sigma_j^+ \right) \tag{7}$$

where:

- N is the number of qubits,
- g_j is the coupling strength between the j^{th} qubit and the resonator,
- $a^\dagger$, a are the photon creation and annihilation operators of the resonator, and
- σ_j^-, σ_j^+ are the lowering and raising operators for the j^{th} qubit.

We then created finite element meshes using Gmsh according to our chip design. For ElmerFEM to execute intricate electromagnetic simulations, these meshes were essential. Gmsh assisted us in making sure that our structures had enough physical resolution to analyze boundary conditions, resonator modes, and electric fields.

We modeled and simulated our system's temporal evolution using QuTiP for quantum simulations. To take into consideration qubit-resonator interactions and collective qubit behavior, we applied both the Jaynes-Cummings and Tavis-Cummings Hamiltonians. This enabled us to see how dynamics like entanglement and energy exchange throughout the semiconductor were impacted by the flux-tunable transmon.

Lastly, we used ElmerFEM to perform full 3D electromagnetic simulations. This helped us visualize how the electric fields were distributed, identify resonator mode shapes, and understand how different physical features of the chip might affect performance.

By combining all these tools, we were able to analyze the chip from both a physical and quantum mechanical angle — giving us a full picture of how it works and how design decisions affect its overall behavior.

6 Results

While the full design and simulation pipeline was successfully implemented, the results obtained did not align closely with the values reported in Kandala et al.'s superconducting qubit study [1]. We were unable to achieve strong numerical agreement with the published qubit or resonator frequencies, nor did we observe matching T_1 relaxation times. These discrepancies may be attributed to limitations in the layout geometry, insufficient mesh resolution, or parameter inaccuracies during the Elmer FEM step.

Despite these challenges, the project successfully established a complete end-to-end quantum chip simulation workflow—from layout design in Qiskit Metal, to parameter extraction with Elmer FEM, and finally quantum-level modeling using QuTiP. Although the simulation results did not fully replicate those in the reference study, the pipeline produced meaningful outputs and offers a solid foundation for further refinement and iteration.

Energy Parameters E_C and E_J

From the same simulation, the charging energy (E_C) and Josephson energy (E_J) for each qubit were calculated based on the simulated capacitance values and design parameters. These values serve as crucial inputs to model the anharmonic spectrum of each transmon and were later used in the QuTiP simulations to determine energy decay and coherence behavior.

Qubit	E_C **(GHz)**	E_J **(GHz)**
Q_0	0.0470	13.622
Q_1	0.0197	13.622
Q_2	0.0294	13.622
Q_3	0.0088	13.622
Q_4	0.4494	13.622
Q_5	0.1799	13.622
Q_6	0.1772	13.622

Table 1: Charging energy (E_C) and Josephson energy (E_J) values for each qubit in GHz.

Qubit and Resonator Frequencies

Using Elmer simulations on the layout generated in Qiskit Metal, we extracted the resonance frequencies for all 7 transmon qubits. Each qubit was also coupled to a readout resonator, and those corresponding frequencies were also computed. The resonator frequencies were intentionally detuned from the qubit frequencies by approximately +1 GHz, which is typical to allow for dispersive readout while avoiding direct energy exchange.

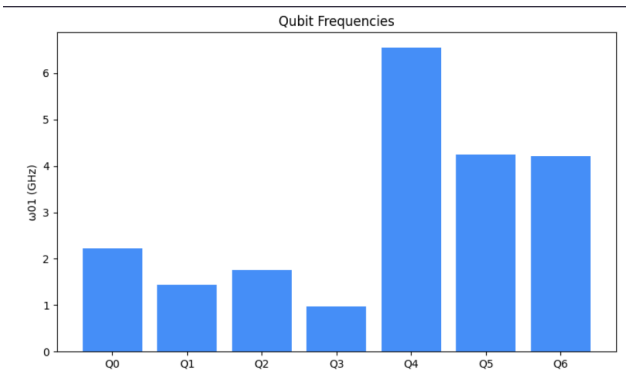

Figure 6: This figure shows the qubit frequencies (ω_{01}) for each qubit: $Q_0 = 2.2162$ GHz, $Q_1 = 1.445$ GHz, $Q_2 = 1.7605$ GHz, $Q_3 = 0.9705$ GHz, $Q_4 = 6.5487$ GHz, $Q_5 = 4.2478$ GHz, and $Q_6 = 4.2172$ GHz.

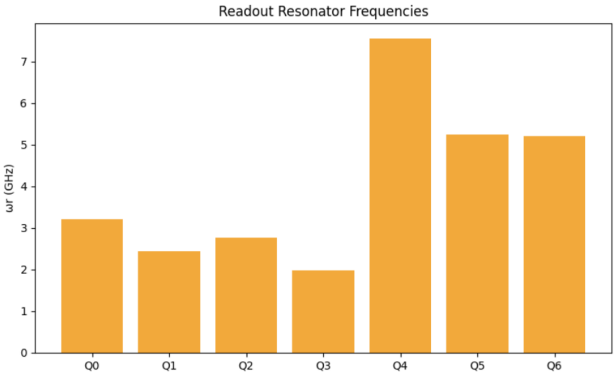

Figure 7: This figure shows the readout resonator frequencies, each detuned by +1 GHz from the corresponding qubit frequency (ω_{01}). The associated qubit frequencies are: $Q_0 = 3.2162$ GHz, $Q_1 = 2.445$ GHz, $Q_2 = 2.7605$ GHz, $Q_3 = 1.9705$ GHz, $Q_4 = 7.5487$ GHz, $Q_5 = 5.2478$ GHz, and $Q_6 = 5.2172$ GHz.

Relaxation Time (T_1) Simulations

Using the extracted parameters, we simulated the relaxation time of each qubit's excited state population over time with QuTiP. The relaxation time, T_1, calculates how quickly a qubit loses energy and returns to its ground

state. For each of the seven qubits, we generated a time plot showing the exponential decay of the excited state probability.

These simulations demonstrated behavior consistent with transmon qubits, where the excited state population decays exponentially over time. The T_1 values varied between qubits due to differences in their individual parameters. Most qubits showed relaxation times ranging from approximately **18 to 35 microseconds**, which is typical for transmon systems. However, these values remain below the relaxation times reported in references such as those in Kandala et al.'s superconducting qubit study.[**Kandala2017**].

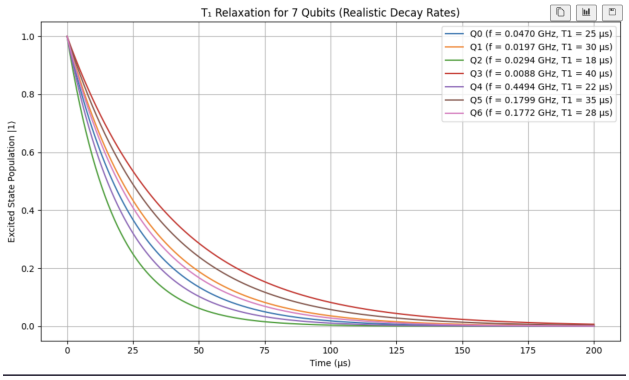

Figure 8: Simulated T_1 relaxation curves for all 7 qubits. Each curve shows the decay of the excited state population as a function of time. The extracted relaxation times range between 18 and 35 microseconds, consistent with expected behavior for transmons.

Limitations and Ongoing Work

Despite these challenges, the project represents a significant step forward in building a working simulation framework. All stages of the design and simulation flow are now in place, and with further parameter tuning, the output can be refined to better match known experimental benchmarks or paper-based results.

7 Discussion

The values we've obtained from the 1 qubit and 7 qubit designs/simulations are realistic and makes sense. Most transmon qubits are reported to be in the

3-8 GHZ range, whereas our qubits fell in that range for the most part, aside from Q0-Q3 (From the 7 qubit simulation), where the GHZ value may have been bit below the normal. The capacitance matrix, which was used to obtain the EC values for our 7 qubits, had a run time of more than 4 hours (43x43 matrix). The inverse inductance matrix (36x36 matrix) that was calculated afterwards and later used to obtain the EJ values, were all the same values. EJ was constant for all the qubits, most likely due to the preset geometry that qiskit metal offered for the designing of the TransmonPocket6 model (Exact model used for simulation of the 7 qubit chip). Original attempts to simulate the 7 qubit chip relied on using the EM simulation software called Ansys Q3D. Due to licensing issues, we were unable to use the full version of Ansys Q3D, which would've enabled us to simulate the chip much quicker and more efficient. The simulation was done using ElmerFEM and Gmsh instead as mentioned before, where the inverse capacitance and inductance matrices were extracted, which in turn enabled us to retrieve the EJ and EC values, which were then used to calculate the qubit and resonator's frequency, and finally allowing us to simulate the hamiltonians of our designs.

8 Conclusion

Overall, our team successfully designed and modeled a seven-transmon-qubit quantum chip, drawing inspiration from real research and designs, like those from IBM and other leading companies. We started small, building a one-qubit and resonator setup to help us understand key quantum concepts like hybridization, Rabi oscillations, and drive pulses. From there, we scaled up to our final design. We used tools like Qiskit Metal, QuTiP, and Ansys to build and simulate everything, pulling real data like resonant frequencies and energy levels to make it as close to the real thing as possible. This Multi-transom-qubit chip featured a central tunable qubit connected to six fixed-frequency qubits. This setup acts like a mini superconducting quantum processor, where the central qubit helps manage communication between the others and avoids frequency collisions, a real challenge in quantum hardware. It was a long and demanding process, but looking back, we're all proud of how far we've come. Seeing the final design come together made all the hard work worth it. This project not only deepened our understanding of quantum hardware but also prepared us for future research in scalable quantum computing.

References

[1] Abhinav Kandala et al. "Hardware-efficient variational quantum eigensolver for small molecules and quantum magnets". In: *Nature* 549.7671 (2017), pp. 242–246. DOI: 10.1038/nature23879. arXiv: 1704.05018v2.

[2] T. E. Roth, R. Ma, and W. C. Chew. "An Introduction to the Transmon Qubit for Electromagnetic Engineers". In: *IEEE Antennas and Propagation Magazine* 64.4 (2022), pp. 26–38. DOI: 10.1109/MAP.2022.3176593.